

UO₂ nanoparticles synthesis from leaching solutions on the hematite support

Zygmunt Sadowski* and Aleksandra Skłodowska

*Wrocław University of Technology,
Wybrzeże Wyspiańskiego 27, 50-370 Wrocław
email: zygmunt.sadowski@pwr.edu.pl

In the present studies the bacterial leaching process is used to extract uranium from the uranium mining wastes. The bioleaching process is environment friendly and gives the extraction yield of over 90%. The bioleaching solutions were obtained from the waste materials located at different places at Lower Silesia (Kowary, Grzmiąca, Kopaniec). Among various templates the hematite Fe₂O₃ nanoparticles are most useful. Interactions uranium ions with synthesized nanoparticles of hematite, magnesite, and iron were examined.

1. INTRODUCTION

The rising global demand of various metal in the past few decades has forced to use the solid tailings as potential new sources. To respond to these challenges the uranium mining wastes, located at Lower Silesia (POLAND) were treated as new uranium resources. The uranium exploration and exploitation in the South-West Poland (Lower Silesia District) was carried out since 1925 when the first 9 tons of uranium ore were mined of which 690 mg of radium was extracted and mining was developed to 1962 and about 704 tons of U was derived [1].

Bioleaching is a microbiological process of metals dissolution from their mineral sources. Microorganisms are able to mobilize metal by the three ways: acidolysis, complexolysis, and redoxolysis [2]. From the

chemical point of view bioleaching is a biooxidation process. The uranium low-grade ores or wastes bioleaching can be realized by direct or indirect mechanisms (Fig. 1).

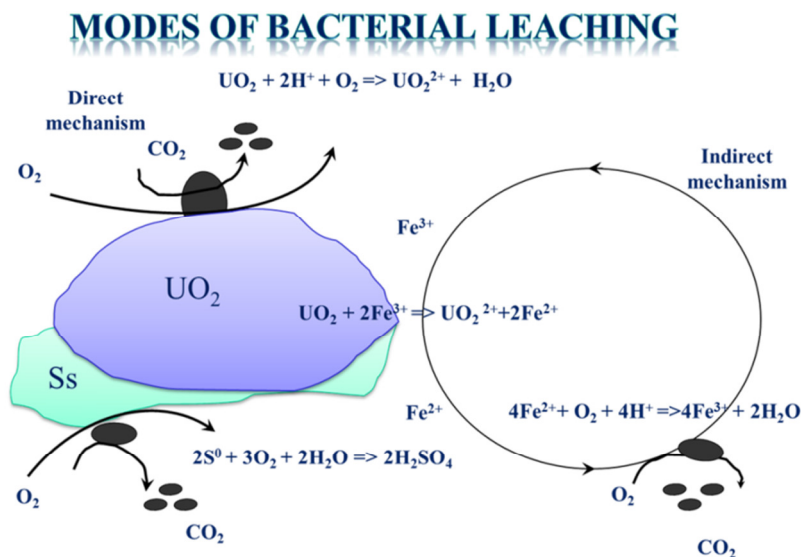


Fig. 1. Direct and indirect uranium bacterial leaching.

The method for the recovery of uranium ions from leaching solution can be UO_2 reductive precipitation. Under anaerobic conditions in the presence of bacteria and organic compounds, bacteria reduces U(VI) to U(IV) through metabolic activity. A number of microorganisms such as *Shewanella oneidensis*, *Shewanella algae*, *Geobacter metallireducences*, *Desulfovibrio desulfuricans* are able to reduce of metal ions [3]. Bioreduction of U(VI) can be coincided with uranyl cation UO_2^{2+} reduction by ferrous iron [4].

Generally, iron oxide nanoparticles play a major role in the sorption and reduction of uranium ions (Fig. 2). The reduction of U(VI) by solid-bound Fe^{2+} ions on hematite is a potentially important pathway for uranium(IV) immobilization. The addition of Fe^{2+} ions to the hematite suspension resulted in reduction of U(VI) to U(IV).

In this work, we demonstrate the application of hematite, magnetite and iron nanoparticles or colloid particles for the treatment of acid bioleaching solutions containing uranium(VI) cations. The adsorption of uranium ions onto the solid surface is a first step to uranium(VI) immobilization. Reductive precipitation of U(VI) at the surface is connected with the electron transfer between Fe(II) and U(VI). Generally,

U(VI) reduction has been observed at the iron-reducing conditions. Thus, it is of great importance to characterize the adsorption and reduction processes, which lead to UO₂ nanoparticle synthesis onto the solid surfaces.

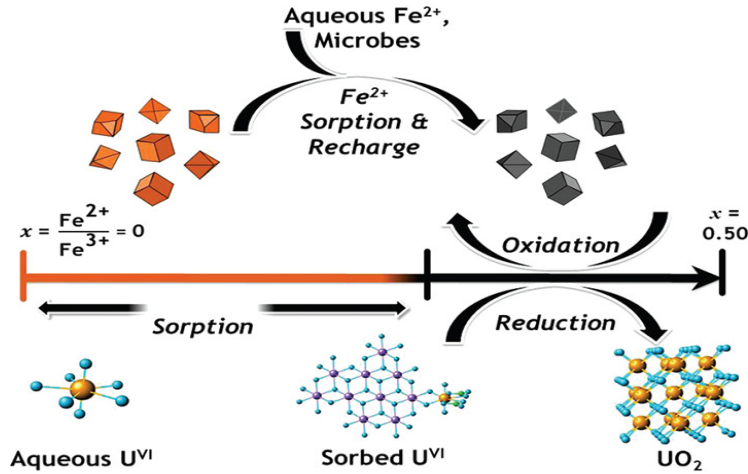


Fig. 2. The effect of Fe²⁺ ions on the U(VI) reduction to UO₂ [10]

2. MATERIALS AND METHODS

All chemical reagents used to the synthesis of iron oxide nanoparticles were of analytical grade.

2.1. Hematite nanoparticles synthesis

Hematite (α -Fe₂O₃) is the most stable iron oxide under ambient. For this reason, it has increasing conditions interest as support material. Hematite nanoparticles were synthesized via hydrolysis method [5]. The particle size of hematite was determined by NICOMP Particle Sizing apparatus (Fig. 3). The average particle size of the synthesized hematite particles was 48.5 nm.

2.2. Magnetite synthesis

Magnetite is generally prepared by precipitation of aqueous solution of Fe²⁺/Fe³⁺ (mole ratio of 1:1) in the presence of a base. The formation of magnetite nanoparticles requires both ferrous and ferric ions. 0.17 g of FeSO₄ 7H₂O and 0.27 g of FeCl₃ 6H₂O were solved in 200 ml aqueous solution, and 1.5 mol/l ammonium hydroxide was dropped.

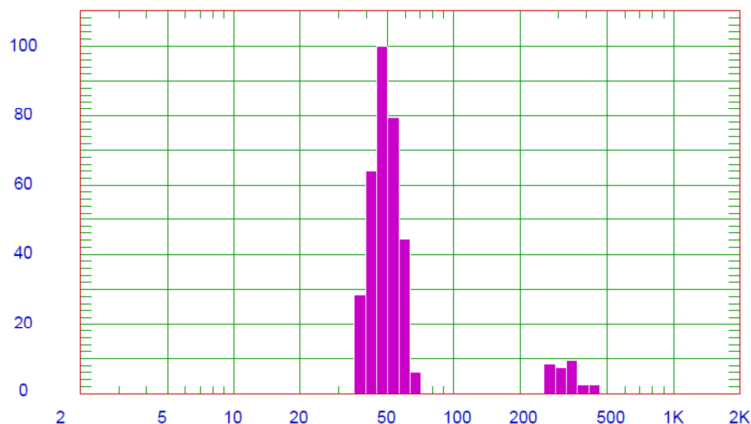
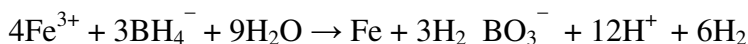


Fig. 3. The size distribution of hematite nanoparticles

2.3. Synthesis of zero-valent iron particle

Zero-valent iron particles were prepared in aqueous solution via the reduction of ferric iron (Fe(III)) with borohydrate [6]. The process can be described according to following reaction:



The borohydride solution was slowly added into the iron chloride during vigorous stirring.

Preliminary characterization of particles using Mastersizer (Malver) apparatus indicated that only hematite particles have nano size. Magnetite and zero-valent iron particles were determined as generally larger in size, with approximately size distributions of 2.5–23 and 4–15 µm, respectively (Fig. 4).

2.4. Bioleaching procedure

The microorganism used in bioleaching study was from Warsaw University collection. Prior to bioleaching tests, the strain was revitalized in freshly prepared 9K medium. Bioleaching was very fast after 20 days of starting the experiment.

2.5. Zeta potential

Zeta potential measurements were conducted using the commercially available equipment Zetasizer from Malveren. The measurements were performed at the constant ionic strength ($1 \cdot 10^{-3}$ M NaCl).

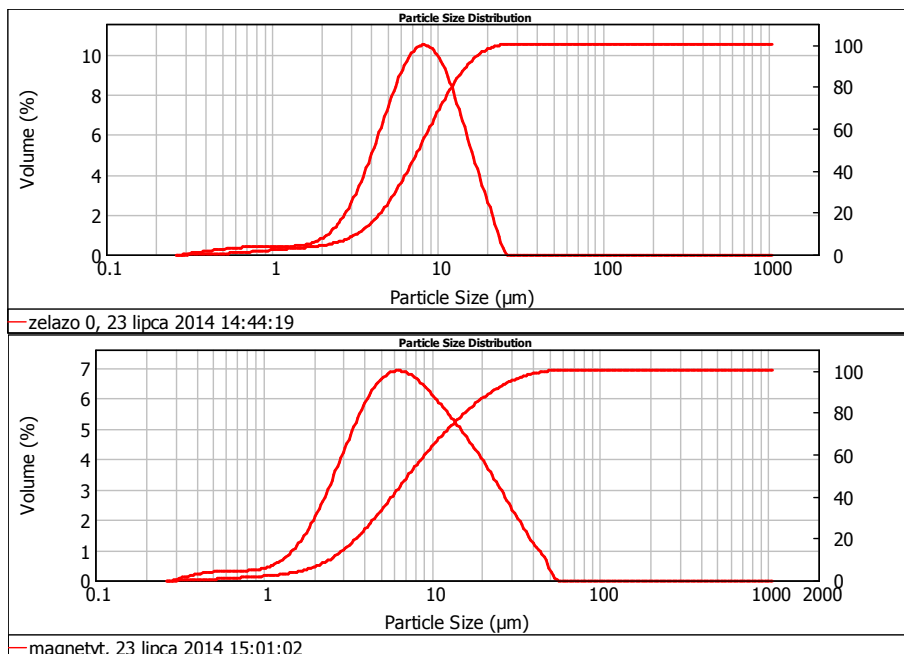


Fig. 4. Size distribution of iron (A) and magnetite (B) particles.

3. RESULTS AND DISCUSSION

The significant U(VI) adsorption capacity onto iron oxides and hydroxides was evidenced. The presented results (Table 1.) showed that the best adsorption was on the magnetite particles. The literature data [7] indicated that adsorption capacity of hematite was affected by the pH. The adsorption capacity of hematite is lower when the range of pH is between 3 and 4.5 and it increases with increase of the pH.

Table 1. Adsorption capacity of U(VI) on iron and iron compounds.

Compounds	U(VI) adsorption capacity [mg/g]	References
Fe ₂ O ₃	34.7 (pH = 7)	[8]
Fe ₃ O ₄ on SiO ₂	52.3 (pH = 6)	[9]
Fe ⁰	21.8 (pH = 7)	[10]
FeOOH	10.68 (pH 7.3–7.8)	[11]

The results of zeta potential measurements of hematite nanoparticles showed that at the ionic strength equals 10^{-3} M NaCl, the average zeta potential was $+32.4 \pm 3.5$ mV at pH = 2.6. The interaction of hematite nanoparticles with the bioleaching solutions led to decrease of positive zeta potential to the value of 6.4 ± 2.7 mV. A decrease of positive value of zeta potential of hematite at the pH range 1–8 is due to adsorption of uranium(VI) ions from leaching solution. The leaching solutions were obtained from bioleaching Kowary (U2) and Grzmionca (U1) solid wastes. The adsorption UO_2^{2-} ions causes a shift of iep to the pH = 5 and pH = 6.

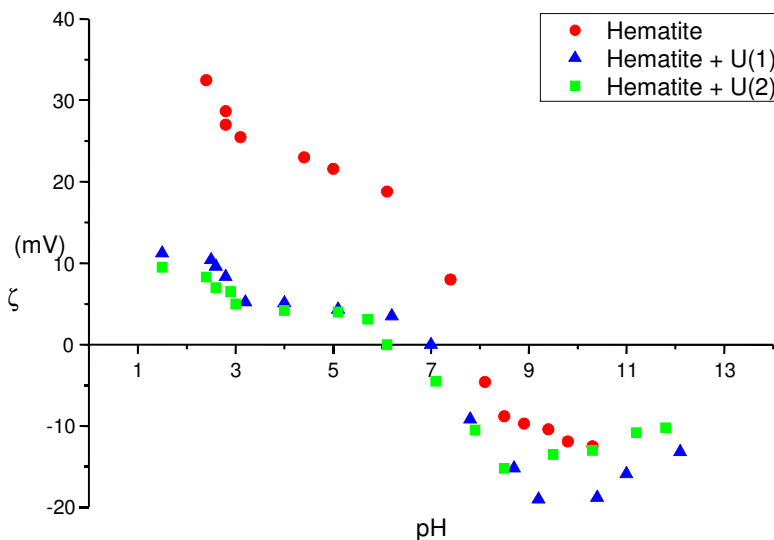


Fig. 5. Zeta potential of hematite particles before and after uranium ions adsorption.

The existing of Fe^{2+} ions on the hematite surface causes the reduction of U(VI) to U(IV) happens [12]. The initial reaction system contained excess of Fe^{2+} ions which were used to reduce of U(VI). The reduction of U(VI) occurred at pH at the vicinity of pH = 2.4. The colloid particles of hematite with UO_2 nanoparticles were obtained. The figure 6 presents a hematite particle with the precipitated UO_2 nanoparticles.

The uranium reduction is most rapid at pH 7.5. The precipitation of UO_2 fits the pseudo-first order rate model [13]. The significant adsorption capacity of U(VI) onto iron oxide and hydroxides (goethite, hematite, and magnetite) was decided at the literature [14, 15]. The sorption of U(VI) onto the hematite surface at the acid range pH was connected with the electrostatic interactions.

Nano-hematite particles have shown to be highly effective for removal of uranium ions from the leaching solutions. The adsorption of uranium was connected with the redox reaction resulting in the chemical reaction of U(VI) to U(IV) on the hematite surface. Fig. 6 presents the hematite particle with adsorbed and reduced uranium ions.

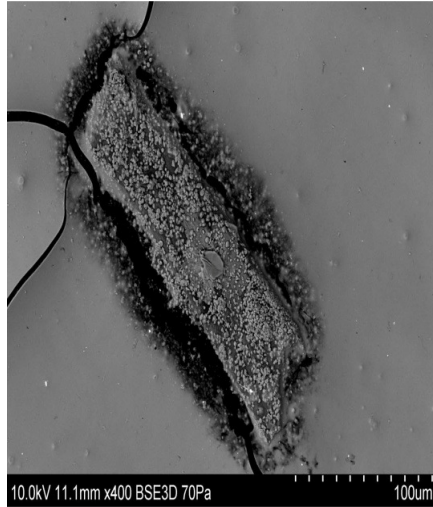


Fig. 6. SEM image of hematite particle with UO₂ nanoparticles on the surface.

X-ray microanalysis is introduced as a tool to evaluate dispersion of UO₂ on the surface of hematite particle. The elemental composition of the samples was obtained by a data collection at 5 windows on the particle surface. On the Figure 7 the image of particles of hematite is with marked areas in which they made analysis.

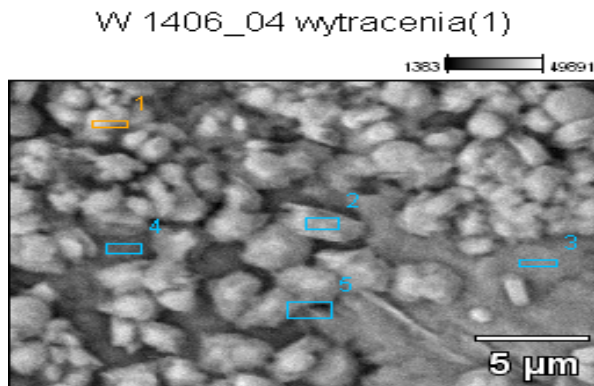


Fig. 7. SEM of hematite particles with the areas of analyses.

The main results of X-ray microanalysis are presented at the Table 2. At the all areas of investigation small quantity of uranium were observed. These data support the synthesis of UO_2 nanoparticles on the hematite surface

Table 2. Chemical composition of the hematite particles and uranium nanoparticles [weight %].

	O-K	Na-K	Al-K	Si-K	Fe-K	U-M
Area-1	74.85		0.35	0.36	10.21	0.07
Area-2	76.93			0.25	9.02	0.05
Area-3	52.50		0.30	0.33	7.92	0.01
Area-4	11.8	0.14	0.12	0.08	3.19	0.03
Area-5	35.81	0.26	0.20	0.31	6.64	0.07

4. CONCLUSION

1. Hexavalent uranium U(VI) can be reduction by Fe(II) bearing materials. The corrosion products of iron are responsible for the U(VI) reduction.
2. The nanoparticles of UO_2 were formed from reduction of U(VI) by Fe^{2+} ions on the hematite nanoparticles.
3. The adsorption of UO_2^{2+} ions onto the hematite surface caused a decrease of zeta potential values.

ACKNOWLEDGEMENTS

The work was financed by a statutory activity subsidy from the Polish Ministry of Science and Higher Education for the Faculty of Chemistry of Wroclaw University of Technology.

REFERENCES

- [1] W. Adamski „Wpływ pouranowych wyrobisk górniczych na środowisko człowieka” [in:] „Człowiek Środowisko Zagrożenia” M. Zdulski (Ed.), Wydawnictwo Nauczycielskie, Jelenia Góra, (2000).
- [2] L. Newsome, K. Morris, R. Lloyd, *Chemical Geology*, **363**, 164-184, (2014).
- [3] E. Marsili, H. Beyenal, L. Di Palma, C. Merli, A. Dohnalkova, J. E. Amonette, Z. Lewandowski, *Environ. Sci. Technol.*, **41**, 8349-8354 (2007).
- [4] T. Behrends, P. Van Cappellen, *Chemical Geology*, **220**, 315-327, (2005).
- [5] T. P. Raming, A. J. A. Winnubst, C. M. Kats, A.P. Philipse, *J. Colloid Interface Sci.*, **249**, 346-350, (2002).
- [6] S. (Doyurum) Yusan, S. (Akyil) Erenturk, *Desalination*, **269**, 58-66, (2011).
- [7] X. Shuibo, Z. Chun, Z. Xinghuo, Y. Jing, Z. Xiaojian, W. Jingsong, *J. Environmental Radioactivity*, **100**, 162-166, (2009).
- [8] D. Das, M. K. Sureshkumar, S. Koley, N. Mithal, O. G. S. Pillai 2010, *J. Radioanal. Nucl. Chem.*, **285**, 447-454, (2010).
- [9] F-L. Fan, Z. Qin, J. Bai, W-D. Rong, F-Y. Fan, W. Tian, X-L. Wu, Y. Wang, L. Zhao, *Journal Environmental Radioactivity*, **106**, 40-46, (2012).
- [10] D. E. Latta, C. A. Gorski, M. I. Boyanow, E. J. O’Loughlin, K. M. Kemner, M. M. Scherer, 2012, *Environ. Sci. Technol.*, **46**, 778-786 (2012).
- [11] H. Zeng, D. E. Giammar, *J. Nanopart Res.*, **13**, 3741-3754, (2011).
- [12] Y-P. Sun, X-q. Li, J. Cao, W-x. Zhang, H.P. Wang, *Advances Colloid Interface Science*, **120**, 47-56, (2006).
- [13] G. Zhang, J. M. Senko, S. D. Kelly, H. Tan, K. M. Kemner, W. D. Burgos, *Geochimica Cosmochimica Acta*, **73**, 3523-3538, (2009).
- [14] R. A. Crane, M. Dickinson, I. C. Popescu, T. B. Scott, *Water Research*, **45**, 2931-2942, (2011).
- [15] S. Klimkova, M. Cernik, L. Lacinova, J. Filip, D. Jancik, R. Zboril, *Chemosphere*, **82**, 1178-1184, (2010).

